Available online at http://scik.org

Commun. Math. Biol. Neurosci. 2026, 2026:64

https://doi.org/10.28919/cmbn/9982

ISSN: 2052-2541

THE PREY-CARRION-EATER SYSTEM'S DYNAMICS IN THE PRESENCE OF A SUBSIDY: THE ROLE OF PANIC AND THE GROUP'S HUNTING

DOUAA KHUDHEYER ABID, RAID KAMEL NAJI*

Department of Mathematics, College of Science, University of Baghdad, Baghdad, Iraq.

Abstract: In ecology, the group's hunting behavior and panic are both significant topics. Therefore, a novel three-dimensional dynamical model that integrates carrion availability, a panic-regulated prey population, and a carrion-eater species that simultaneously exploits both subsidy (or carrion) and live prey is proposed and studied. The model incorporates nonlinear functional responses, panic-driven suppression of prey growth, and cooperative hunting in the carrion-eater. Mathematical analysis establishes positivity and boundedness of all state variables, ensuring ecological feasibility. Equilibrium points are explicitly derived, and their local stability is analyzed using the Jacobian matrix, while global stability is assessed through the construction of appropriately designed Lyapunov functions. The results indicate that increasing panic intensity can suppress prey abundance and stabilize the system. At the same time, cooperative hunting enhances the efficiency of carrion-eaters, potentially leading to persistent cohabitation or oscillatory dynamics depending on parameter regimes. These findings extend classical carcass–prey–carrion-eater frameworks, highlighting the critical role of carrion recycling and behavioral mechanisms in shaping multi-trophic ecological dynamics. The model offers a unified theoretical framework for investigating realistic ecosystems where carrion use, panic effects, and mixed feeding strategies combine.

Keywords: panic; the group's hunting, stability; bifurcation; persistence.

2020 Subject Classification: 92D30; 34D20; 34C23.

*Corresponding author

E-mail address: raid.naji@sc.uobaghdad.edu.iq

Received May 15, 2026

1. INTRODUCTION

Prey-predator interactions have long been seen through the prism of direct death in the traditional paradigm of ecology: predators kill prey, which lowers their population, and are then controlled by the availability of this food source [1-3]. This framework offers a basic yet condensed picture of trophic dynamics and is crystallized in fundamental models like the Lotka-Volterra equations. However, a rising body of research in recent decades has transformed this thinking by showing that the mere presence of a predator can cause significant physiological and behavioral changes in prey, a phenomenon known as panic (or fear) [4-6].

According to Wang et al. [7] and Wang and Zou [8], panic of predation causes prey to change their habitat choices, foraging schedules, and vigilance levels. These non-lethal costs have the same capacity to influence population dynamics and ecological structure as direct consumption. Many researchers have since studied the role of panic in the dynamics of ecological systems; see [9-11]. At the same time, research on predator behavior has shifted from focusing on lone hunters to recognizing the frequency and significance of cooperative hunting, in which predators cooperate to catch prey, boosting their effectiveness and allowing them to kill larger or more difficult game [12-14]. Although these developments have greatly enhanced prey-predator theory, the carrion-eaters, a crucial but historically understudied guild, are affected further down the food chain. Organisms that depend entirely or partially on carrion, or animal carcasses, are known as carrion-eaters, and they are crucial to the health of ecosystems [9, 15-17]. By quickly eating carcasses, they reduce the transmission of illness, aid in the cycling of nutrients, and offer a vital subsidy that sustains a variety of communities [18-19]. Carrion's introduction into an ecosystem is not an exogenous or random occurrence; rather, it is inextricably related to the hunting habits and effectiveness of predators. The dynamics of the carrion-eater subsystem must thus be drastically changed by any factor that alters predator efficiency and prey behavior, such as panic effects and cooperative hunting [20-22].

The quantity, quality, spatial distribution, and temporal availability of this resource are determined by the direct killing rate of predators and the non-lethal panic effects on prey, which impact prey condition, spatial aggregation, and vulnerability. The group’s hunting increases per-predator kill rates, often for larger-bodied prey, resulting in larger, more nutrient-rich corpses, which directly amplifies the initial impact [23-25]. However, panic induced by highly successful, cooperative groups may also raise anti-predator reactions in prey, which may ultimately reduce predation rates if prey become too evasive or stressed, or increase them if panic leads to chaotic

herd behavior that predators can exploit [12, 23, 26-27]. The result is a faint, varying pulse of carrion entering the system. Therefore, this research provides a novel carcass-prey-carrion-eater system, a complex, tritrophic feedback loop, to better understand the dynamics of an ecological model in the presence of panic, the group's hunting, and carrion-eaters. In this system, predators are the primary producers of the carrion-eater's resource, which is carcasses. Understanding this interwoven system is more than simply an intellectual exercise because it has immediate implications for ecological management and conservation. The global decline of apex predators and specialized carrion-eaters like vultures, along with human-induced landscape alteration, is upsetting these delicately regulated interactions [28]. Carcass accumulation, increased disease risk, and altered nutrient cycles occur when efficient carrion-eaters vanish [29-30]. On the other hand, hyper-herbivory and changed vegetation dynamics (ecological release) may arise from the loss of panic effects. Human hunters and livestock systems also add new "predators" and "carcass sources" into this network, with complex and often destabilizing outcomes.

In light of the aforementioned, Abid and Naji [15] recently proposed and investigated a unique ecological model that incorporates corpses, prey, and carrion-eaters under the effects of predator-dependent refuge and panic. However, given the significance of this trait for the environment, our earlier model is incorporated into this research, with the group's hunting used in place of predator-dependent refuge.

2. MATHEMATICAL MODEL FORMULATION

This section presents a mathematical formulation of the movement behavior of the carcass-prey-carrion-eater system under the influence of prey panic and carrion-eater cooperation during hunting. Consequently, the dynamics of such a real-world system are formulated using the following theories:

1) Consider $C(T), X(T)$, and $Y(T)$ as the number of carcasses (or resource subsidies), prey, and carrion-eaters at time T. In the absence of carrion-eaters and prey, it is believed that carcasses degrade exponentially with a natural decay rate $d_1 > 0$. Nevertheless, the carrion-eater attacks it using a Lotka-Volterra-type functional response, with a maximum attack rate of $a_1 > 0$, where Λ is the total number of carcasses.
2) The prey's dread of a carrion-eater, symbolized by $h \geq 0$, affects its growth rate (r). An intraspecific competition rate of $b_1 > 0$ indicates that members of the prey population compete within their own species. Its rate of natural death is $d_2 > 0$.

3) It is hypothesized that the carrion-eater consumes prey based on the Lotka-Volterra functional response, which is impacted by the carrion-eater's capacity for cooperative hunting. Therefore, the cooperative term can increase the assault rate (let's say $a_2 > 0$) to $(a_2 + b_2Y)$, where $b_2 \geq 0$ represents the carrion-eater cooperation hunting rate.
4) Furthermore, the natural death rate of the scavenging species is $d_3 > 0$. With conversion rates of $0 < e_1 < 1$ for prey and $0 < e_2 < 1$ for corpses, the functional response of Lotka-Volterra-type explains how the Carrion-eater consumes prey and carcasses in accordance with the mass-action law.

Therefore, it is possible to express the dynamics of this model mathematically as:

$$\begin{aligned} \frac{dC}{dT} &= \Lambda - d_1 C - a_1 CY, \\ \frac{dX}{dT} &= \frac{rX}{1+hY} - d_2 X - b_1 X^2 - (a_2 + b_2 Y)XY, \\ \frac{dY}{dT} &= e_1(a_2 + b_2 Y)XY + e_2 a_1 CY - d_3 Y, \end{aligned} \tag{1}$$

with initial circumstances, $C(0) > 0$, $X(0) > 0$ and $Y(0) > 0$. Although Table 1 describes the parameters.

Table 1: Description of the parameters

Parameters	**description**
Λ	Total number of carcasses
$r > 0$	The birth rate of X
$h \geq 0$	The panic level
$d_1 \in (0,1)$	The death rate of C
$d_2 \in (0,1)$	The death rate of X
$d_3 \in (0,1)$	The death rate of Y
$a_1 > 0$	The attack rate of C
$a_2 > 0$	The attack rate of Y
$b_1 > 0$	The competition rate within X
$b_2 > 0$	The group's hunting rate of Y
$e_1 \in (0,1)$	The rate of conversion from X biomass into Y biomass
$e_2 \in (0,1)$	The rate of conversion from C biomass into Y biomass

Now, reformulate system (1). It becomes:

$$\begin{aligned} \frac{dC}{dT} &= f_1(C, X, Y), \\ \frac{dX}{dT} &= X f_2(C, X, Y), \\ \frac{dY}{dT} &= Y f_3(C, X, Y), \end{aligned} \tag{2}$$

where:

$$f_1(C,X,Y) = \Lambda - d_1C - a_1CY.$$

$$f_2(C,X,Y) = \frac{r}{1+hY} - d_2 - b_1X - (a_2 + b_2Y)Y.$$

$$f_3(C,X,Y) = e_1(a_2 + b_2Y)X + e_2a_1C - d_3.$$

The positivity and boundedness of the system's (2) solutions are established in the net theorem.

Theorem 1. Under the initial circumstances $C(0) = C_0 > 0$, $X(0) = X_0 > 0$, and $Y(0) = Y_0 > 0$, the solutions $(C(T), X(T), Y(T))$ of the system (2) are positive for all $T > 0$, and uniformly bounded.

Proof: For the given initial circumstances, it is acquired:

$$C(T) > C_0\, exp\left(-\int_0^T (d_1 + a_1Y(s))\, ds\right) > 0.$$

$$X(T) > X_0\, exp\left(-\int_0^T \left(d_2 + b_1X(s) + \left(a_2 + b_2Y(s)\right)Y(s)\right)ds\right) > 0.$$

$$Y(T) > Y_0\, exp\left(-\int_0^T (d_3)ds\right) > 0.$$

As a result, every solution that begins inside the first octant stays there forever.

Moreover, the first equation of system (2) leads to:

$$\frac{dC}{dT} \leq \Lambda - d_1C.$$

Thus, due to Lemma 2.1 [31], it is acquired that:

$$C(T) \leq \frac{\Lambda}{d_1}\left[1 + \left(\frac{d_1}{\Lambda}C_0 - 1\right)e^{-d_1T}\right].$$

Hence, as $T \to \infty$, then $C(T) \leq \frac{\Lambda}{d_1}$. Using the second equation, it is acquired that:

$$\frac{dX}{dT} \leq \frac{rX}{1+hY} - d_2X - b_1X^2 \leq X(r - d_2 - b_1X)$$

$$\leq (r - d_2)X\left(1 - \frac{1}{\frac{r-d_2}{b_1}}X\right)$$

Therefore, from Lemma 2.2 [31], it is acquired that:

$$X(T) \leq \frac{r-d_2}{b_1}\left[1 + \left(\frac{r-d_2}{b_1}{X_0}^{-1} - 1\right)e^{-(r-d_2)T}\right]^{-1},$$

which leads to $X(T) \leq \frac{r-d_2}{b_1}$, when $T \to \infty$.

Define $\rho(T) = \frac{e_2}{e_1}C + X(T) + \frac{1}{e_1}Y(T)$, consequently, the derivative with respect to time leads to:

$$\frac{d\rho(T)}{dT} = \frac{e_2}{e_1}\Lambda - \frac{e_2}{e_1}d_1C + \frac{rX}{1+hY} - d_2X - b_1X^2 - \frac{1}{e_1}d_3Y.$$

Therefore, it is acquired that:

$$\frac{d\rho(T)}{dT} \leq \frac{e_2}{e_1}\Lambda + r\left(\frac{r-d_2}{b_1}\right) - \mu\left(\frac{e_2}{e_1}C + X + \frac{1}{e_1}Y\right) = \Lambda_1 - \mu\rho(T),$$

where $\mu = min\{d_1, d_2, d_3\}$ and $\Lambda_1 = \frac{e_2}{e_1}\Lambda + r\left(\frac{r-d_2}{b_1}\right)$. According to Lemma 2.1[31], it is acquired that $\rho(T) \leq \frac{\Lambda_1}{\mu}$, when $T \to \infty$. Thus, the proof is complete.

3. STABILITY AND BIFURCATION

Studying local stability analysis in ecological systems is crucial to understanding how ecosystems respond to small shocks close to their equilibrium states. Mathematicians and ecologists can use this method to predict whether a system will stabilize after a minor shock or deviate and possibly result in significant changes like population collapse or ecosystem upheavals. System (2) has a maximum of four nonnegative equilibrium points. Below is a description of the current circumstances and stability analyses.

The carcasses-equilibrium point $P_C = \left(\frac{\Lambda}{d_1}, 0, 0\right)$ of system (2) exists always.

The carrion-eater-free equilibrium point is symbolized by $P_{CX} = (\bar{C}, \bar{X}, 0) = \left(\frac{\Lambda}{d_1}, \frac{r-d_2}{b_1}, 0\right)$, and exists provided that:

$$r > d_2. \tag{3}$$

The equilibrium point without prey is symbolized by $P_{CY} = (\hat{C}, 0, \hat{Y}) = \left(\frac{d_3}{e_2 a_1}, 0, \frac{e_2\Lambda a_1 - d_1 d_3}{a_1 d_3}\right)$, and exists provided that:

$$e_2\Lambda a_1 > d_1 d_3. \tag{4}$$

A special cohabitation equilibrium point $P_* = (C_*, X_*, Y_*)$ exists, where

$$\left.\begin{aligned} C_* &= \frac{\Lambda}{d_1 + a_1 Y_*} \\ X_* &= \frac{d_3(d_1 + a_1 Y_*) - e_2 a_1 \Lambda}{e_1(d_1 + a_1 Y_*)(a_2 + b_2 Y_*)} \end{aligned}\right\}. \tag{5}$$

With Y_* standing for a positive root of a polynomial of fifth order:

$$\sigma_1 Y^5 + \sigma_2 Y^4 + \sigma_3 Y^3 + \sigma_4 Y^2 + \sigma_5 Y^1 + \sigma_6 = 0,$$

where:

$$\sigma_1 = -e_1 b_2^2 a_1 h < 0.$$
$$\sigma_2 = -e_1 b_2 (2a_1 a_2 h + b_2 d_1 h + b_2 a_1) < 0.$$
$$\sigma_3 = -e_1 (2b_2 a_2 d_1 h + a_2^2 a_1 h + 2a_1 a_2 b_2 + b_2^2 d_1 + a_1 b_2 d_2 h) < 0.$$

$$\sigma_4 = -[e_1\left(a_2^2 d_1 h + a_2 d_1 b_2 + a_2 a_1 d_2 h + a_2^2 a_1 + b_2 d_1 h + a_1 b_2 (r - d_2)\right) + b_1 d_3 a_1 h].$$

$$\sigma_5 = -[e_1\left((r - d_2)(a_1 a_2 + b_2 d_1) + a_1 d_1 (d_2 h + a_2)\right) + b_1 d_3 (d_1 h + a_1) - \Lambda \mathrm{h} e_2 b_1 a_1].$$

$$\sigma_6 = e_1 a_1 d_1 (r - d_2) + \Lambda b_2 e_2 a_1 - d_3 b_1 d_1.$$

Therefore, P_* exists uniquely in $int.\mathbb{R}_+^3$ if the following sufficient conditions are met.

$$\frac{e_2 a_1 \Lambda}{(d_1 + a_1 Y_*)} < d_3. \tag{6a}$$

$$e_1 a_1 d_1 r + \Lambda b_2 e_2 a_1 > d_2 e_1 a_1 d_1 + d_3 b_1 d_1. \tag{6b}$$

A long with one set of the next conditions:

$$\left.\begin{matrix} \sigma_4 < 0 \\ or \\ \sigma_5 > 0 \end{matrix}\right\} \tag{7}$$

The linearization method that depends on the Jacobian matrix M at the point (C, X, Y), which may be stated in the following form, might be utilized to perform the local stability analysis of the stated equilibrium sites.

$$M(C, X, Y) = \begin{bmatrix} -d_1 - a_1 Y & 0 & -a_1 C \\ 0 & -b_1 X + f_2 & -X\left(\frac{rh}{(1+hy)^2} + a_2 + 2b_2 Y\right) \\ e_2 a_1 Y & e_1 Y (a_2 + b_2 Y) & e_1 b_2 XY + f_3 \end{bmatrix}, \tag{8}$$

where f_2 and f_3 are given in system (2).

On the other hand, studying the global stability of ecological systems aims to provide a comprehensive understanding of their long-term behavior and resilience. This information is crucial for addressing pressing environmental problems and ensuring the sustainability of the ecosystems on our planet.

Better judgments in ecology, conservation, and resource management are also ensured by the mathematical toolkit that local bifurcation analysis offers for managing and forecasting sudden ecological shifts. By examining bifurcations, ecologists can predict when and why systems might experience significant shifts, preventing unfavorable outcomes like extinctions or ecological collapses. Thus, the phenomenon of local bifurcation in system (2) is investigated in this section.

Now, reformulate system (2) as $\frac{dZ}{dT} = F(Z)$, where $Z = (C, X, Y)^T$ and $F(Z) = (f_1, Xf_2, Yf_3)^T$.

The following is a representation of the universal Jacobian matrix's second directional derivative:

$$D^2 F(\boldsymbol{v}, \boldsymbol{v}) = [\delta_{i1}], \tag{9}$$

where:

$$\delta_{11} = -2a_1v_1v_3.$$

$$\delta_{21} = -2b_1v_2^2 + 2\left(\frac{rh^2X}{(1+hY)^3} - b_2X\right)v_3^2 - 2\left(\frac{rh}{(1+hY)^2} + a_2 + 2b_2Y\right)v_2v_3.$$

$$\delta_{31} = 2e_1b_2Xv_3^2 + 2e_2a_1v_1v_3 + +2(e_1a_2 + 2e_1b_2Y)v_2v_3.$$

However, the third directional derivative is:

$$D^3F(\boldsymbol{v},\boldsymbol{v},\boldsymbol{v}) = [\sigma_{i1}], \tag{10}$$

where:

$$\sigma_{11} = 0.$$

$$\sigma_{21} = \frac{6(1+hY)(h^2r-(1+hY)^3b_2)v_2v_3^2-6h^3rXv_3^3}{(1+hY)^4}.$$

$$\sigma_{31} = 6b_2e_1v_2v_3^2.$$

While $\boldsymbol{v} = (v_1, v_2, v_3)^T$.

Keeping the above in mind, the following theorems can be proved.

Theorem 2. For the carcasses-equilibrium point $P_C = \left(\frac{\Lambda}{d_1}, 0,0\right)$:

1) P_C is locally asymptotically stable if the condition (11) is met, and it's a saddle point otherwise.
2) In addition to condition (11), condition (12) is met. Then P_C becomes a globally asymptotically stable.
3) System (2) demonstrates a transcritical bifurcation (TCB) around P_c, if the parameter d_3 travels vie the value $\frac{e_2a_1\Lambda}{d_1} \equiv \tilde{d}_3$ with $r \neq d_2$.

$$\left.\begin{matrix} r < d_2 \\ e_2a_1\Lambda < d_3d_1 \end{matrix}\right\}. \tag{11}$$

$$\frac{a_1\Lambda}{d_1} < d_3. \tag{12}$$

Proof:**(1)** Direct calculation shows that the eigenvalues of $M(P_C)$, $\lambda_{11} = -d_1$, $\lambda_{12} = r - d_2$, and $\lambda_{13} = \frac{e_2a_1\Lambda-d_3d_1}{d_1}$. Thus, P_C becomes locally asymptotically stable under the condition (11). Furthermore, P_C becomes a saddle point when at least one of the requirements in (11) is broken.

(2) Define the real valued function $\mho_1 = \left(C - C_0 - C_0\ln\frac{C}{C_0}\right) + X + Y$, with $C_0 = \frac{\Lambda}{d_1}$. Direct calculation explains that $\mho_1 : U_1 \to \mathbb{R}$, where $U_1 = \{(C,X,Y) \in \mathbb{R}_+^3, C > 0, X \geq 0, Y \geq 0\}$, hence $\mho_1(P_C) = 0$ and $\mho_1(C,X,Y) > 0, \forall\, (C,X,Y) \in U_1 - P_C$. Straightforward computation leads to:

$$\frac{d\mho_1}{dT} = \left(\frac{C-C_0}{C}\right)\frac{dC}{dT} + \frac{dX}{dT} + \frac{dY}{dT} \leq -\frac{d_1}{C}(C - C_0)^2 - (d_3 - a_1C_0)Y - (d_2 - r)X.$$

Hence, from condition (11) with condition (12), it is concluded that $\frac{d\mho_1}{dT} < 0$. Thus, P_C is globally asymptotically stable.

(3) Eq. (8) at P_c with $d_3 = \tilde{d}_3$, becomes:

$$M(P_c, \tilde{d}_3) = \begin{bmatrix} -d_1 & 0 & -\frac{a_1\Lambda}{d_1} \\ 0 & r - d_2 & 0 \\ 0 & 0 & 0 \end{bmatrix}.$$

Hence, the eigenvalues of $M(P_c, \tilde{d}_3)$ can be written $\lambda_{11} = -d_1 < 0$, $\lambda_{12} = r - d_2$, and $\lambda_{13} = 0$. Define $\tilde{\boldsymbol{v}} = (v_{11}, v_{12}, v_{13})^T$, and $\tilde{\boldsymbol{\psi}} = (\psi_{11}, \psi_{12}, \psi_{13})^T$ as the eigenvectors corresponding to $\lambda_{13} = 0$ for $M(P_c, \tilde{d}_3)$, and $\left[M(P_c, \tilde{d}_3)\right]^T$ respectively. gives that $\tilde{\boldsymbol{v}} = (-\frac{a_1\Lambda}{d_1^2}, 0,1)^T$, and $\tilde{\boldsymbol{\psi}} = (0,0,1)^T$.

Furthermore, a simple calculation using Eq. (9) explains that:

$$\frac{\partial F}{\partial d_3} = F_{d_3} = (0,0,-Y)^T \Rrightarrow \tilde{\boldsymbol{\psi}}^T[F_{d_3}(P_c, \tilde{d}_3)] = 0.$$

$$\tilde{\boldsymbol{\psi}}^T[DF_{d_3}(P_c, \tilde{d}_3)\tilde{\boldsymbol{v}}] = -1.$$

$$\tilde{\boldsymbol{\psi}}^T[D^2F(P_c, \tilde{d}_3)(\tilde{\boldsymbol{v}}, \tilde{\boldsymbol{v}})] = -2e_2\frac{a_1^2\Lambda}{d_1^2}.$$

Hence, a TCB happens in accordance with Sotomayer's theorem [32].

Theorem 3: For the carrion-eater-free equilibrium point $P_{CX} = (\bar{C}, \bar{X}, 0)$:

1) P_{CX} is locally asymptotically stable if the condition (13) is satisfied; otherwise, it is a saddle point.
2) When the condition (14) holds, P_{CX} becomes a globally asymptotically stable.
3) System (2) demonstrates a TCB around P_{CX}, if the parameter e_2 travels vie the positive value $\bar{e}_2 = \frac{b_1d_1d_3 - e_1a_2d_1(r-d_2)}{a_1b_1\Lambda}$.

$$e_2a_1\Lambda b_1 + d_1e_1a_2(r - d_2) < d_3d_1b_1. \quad (13)$$

$$a_1\bar{C} + (b_2Y + a_2)\bar{X} < d_3. \quad (14)$$

Proof: **(1)** The eigenvalues of $M(P_{CX})$ are determined by $\lambda_{21} = -d_1 < 0$, $\lambda_{22} = d_2 - r < 0$, and $\lambda_{23} = \frac{e_2a_1\Lambda b_1 + d_1e_1a_2(r-d_2) - d_3d_1b_1}{d_1b_1}$. Then, P_{CX} is locally asymptotically stable if condition (13) is met. Otherwise, the carrion-eater-free equilibrium point loses its stability, and it becomes a saddle point.

(2) Consider the real valued function $\mho_2 = \left(C - \bar{C} - \bar{C}\, ln\frac{C}{\bar{C}}\right) + (X - \bar{X} - \bar{X} ln\frac{X}{\bar{X}}) + Y$, with $\bar{C} = \frac{\Lambda}{d_1}$ and $\bar{X} = \frac{r-d_2}{b_1}$. Direct calculation reveals that $\mho_2 : U_2 \to \mathbb{R}$, where $U_2 = \{(C, X, Y) \in \mathcal{R}_+^3, C > 0, X > 0, Y \geq 0\}$, so that $\mho_2(P_{CX}) = 0$ and $\mho_2(C, X, Y) > 0, \forall\, (C, X, Y) \in U_2 - P_{CX}$. Furthermore, simple computation yields that:

$$\frac{d\mho_2}{dT} \leq -\frac{d_1}{C}(C - \bar{C})^2 - b_1(X - \bar{X})^2 - [d_3 - a_1\bar{C} - (a_2 + b_2 Y)\bar{X}]Y.$$

Thus, condition (14) yields $\frac{d\mho_2}{dT} < 0$. Accordingly, P_{CX} is globally asymptotically stable.

(3) The system's Jacobian matrix (2) at P_{CX} with $e_2 = \bar{e}_2$ becomes:

$$M(P_{CX}, \bar{e}_2) = \begin{bmatrix} -d_1 & 0 & -a_1\frac{\Lambda}{d_1} \\ 0 & -(r - d_2) & -\frac{(rh+a_2)(r-d_2)}{b_1} \\ 0 & 0 & 0 \end{bmatrix}.$$

Therefore, $\bar{\lambda}_{21} = -d_1$, $\bar{\lambda}_{22} = -(r - d_2)$, and $\bar{\lambda}_{23} = 0$ represent the eigenvalues of $M(P_{CX}, \bar{e}_2)$. Define $\bar{\boldsymbol{v}} = (\bar{v}_{21}, \bar{v}_{22}, \bar{v}_{23})^T$, and $\bar{\boldsymbol{\psi}} = (\bar{\psi}_{21}, \bar{\psi}_{22}, \bar{\psi}_{23})^T$ as the eigenvectors corresponding to $\bar{\lambda}_{23} = 0$ for $M(P_{CX}, \bar{\Lambda})$, and $[M(P_{CX}, \bar{e}_2)]^T$ respectively, then it obtain that $\bar{\boldsymbol{v}} = \left(-\frac{a_1\Lambda}{d_1^2}, -\frac{(rh+a_2)}{b_1}, 1\right)^T$, and $\bar{\boldsymbol{\psi}} = (0,0,1)^T$.

Additionally, straight calculation using Eq. (9) reveals that:

$$\frac{\partial F}{\partial e_2} = F_{e_2} = (0,0,a_1 CY)^T \;\Rrightarrow\; \bar{\boldsymbol{\psi}}^T[F_{e_2}(P_{CX}, \bar{e}_2)] = 0.$$

$$\bar{\boldsymbol{\psi}}^T[DF_{e_2}(P_{CX}, \bar{e}_2)\bar{\boldsymbol{v}}] = \frac{a_1\Lambda}{d_1}.$$

$$\bar{\boldsymbol{\psi}}^T[D^2F(P_{CX}, \bar{e}_2)(\bar{\boldsymbol{v}}, \bar{\boldsymbol{v}})] = 2\bar{e}_2\frac{a_1^2\Lambda}{d_1^2} + 2e_1 b_2\left(\frac{r-d_2}{b_1}\right) + 2e_1 a_2\frac{(rh+a_2)}{b_1} \neq 0.$$

Thus, according to Sotomayor's theorem, there is a TCB.

Theorem 4: For the equilibrium point without prey$P_{CY} = (\hat{C}, 0, \hat{Y})$:

1) P_{CY} is locally asymptotically stable if the condition (15) is satisfied; otherwise, it is a saddle point.
2) When the condition (16) holds, then P_{CY} becomes globally asymptotically stable.
3) If the condition (17) is satisfied, system (2) shows a TCB around P_{CY} if the parameter r travels via the value $\hat{r} = \left[d_2 + \left(a_2 + b_2\hat{Y}\right)\hat{Y}\right]\left(1 + h\hat{Y}\right)$. If not, a pitchfork bifurcation occurs.

$$r < \left[d_2 + \left(a_2 + b_2\hat{Y}\right)\hat{Y}\right]\left(1 + h\hat{Y}\right). \tag{15}$$

$$r < d_2. \tag{16}$$

$$-2b_1 - 2\left(\frac{rh}{(1+h\hat{Y})^2} + a_2 + 2b_2\hat{Y}\right) \neq \left(\frac{e_1(a_2+b_2\hat{Y})(d_1+a_1\hat{Y})}{e_2a_1^2\hat{C}}\right) \tag{17}$$

Proof: **(1)** Direct calculation shows that, for the equilibrium point without prey $P_{CY} = \left(\hat{C}, 0, \hat{Y}\right) = \left(\frac{d_3}{e_2a_1}, 0, \frac{e_2\Lambda a_1 - d_1d_3}{a_1d_3}\right)$, the eigenvalues of $M(P_{CY})$ are determined as:

$$\lambda_{31}, \lambda_{33} = \frac{-(d_1+a_1\hat{Y}) \pm \sqrt{(d_1+a_1\hat{Y})^2 - 4a_1{}^2e_2\hat{Y}\hat{C}}}{2},\ \lambda_{32} = \frac{r}{1+h\hat{Y}} - d_2 - \left(a_2 + b_2\hat{Y}\right)\hat{Y}.$$

Therefore, P_{CY} is locally asymptotically stable if the condition (15) holds. Otherwise, it is an unstable saddle point.

(2) Consider the real valued function $\mho_3 = l_1\frac{1}{2}\left(C - \hat{C}\right)^2 + l_2X + l_3\left(Y - \hat{Y} - \hat{Y}\ln\frac{Y}{\hat{Y}}\right)$, where $\hat{C} = \frac{d_3}{a_1e_2}$, $\hat{Y} = \frac{e_2a_1\Lambda - d_3d_1}{a_1d_3}$, and $l_i, i = 1,2,3$ are positive constants to be determine. Straightforward computation leads to $\mho_3: U_3 \to \mathbb{R}$, where $U_3 = \{(C,X,Y) \in \mathbb{R}^3_+, C \geq 0, X \geq 0, Y > 0\}$, so that $\mho_3(P_{CY}) = 0$ and $\mho_3(C,X,Y) > 0, \forall\ (C,X,Y) \in U_3 - P_{CY}$. Furthermore:

$$\begin{aligned}\frac{d\mho_3}{dT} &= -l_1(d_1 + a_1Y)\left(C - \hat{C}\right)^2 - l_1a_1\hat{C}\left(C - \hat{C}\right)\left(Y - \hat{Y}\right)\\ &\quad + l_2\frac{rX}{1+hY} - l_2d_2X - l_2b_1X^2 - l_2(a_2 + b_2Y)YXY\\ &\quad + l_3e_1(a_2 + b_2Y)X - l_3e_1(a_2 + b_2Y)X\hat{Y} + l_3e_2a_1\left(C - \hat{C}\right)\left(Y - \hat{Y}\right)\end{aligned}.$$

Therefore, selecting the constants as $l_1 = \frac{e_2}{\hat{C}}$, $l_2 = e_1$, and $l_3 = 1$, yield that:

$$\frac{d\mho_3}{dT} \leq -\frac{e_2}{\hat{C}}(d_1 + a_1Y)\left(C - \hat{C}\right)^2 - e_1(d_2 - r)X.$$

According to condition (16), $\frac{d\mho_3}{dT}$ is negative semidefinite. Additionally, since the singleton set $\{P_{CY}\}$ is the only invariant set, which is part of the set of points, that makes $\frac{d\mho_3}{dT} = 0$, then P_{CY} becomes an appealing point using LaSalle's invariance principle. As a result, P_{CY} is asymptotically stable everywhere.

(3) The matrix $M(C,X,Y)$ at P_{CY} with $r = \hat{r}$ can be expressed as:

$$M(P_{CY}, \hat{r}) = \begin{bmatrix} -d_1 - a_1\hat{Y} & 0 & -a_1\hat{C} \\ 0 & 0 & 0 \\ e_2a_1\hat{Y} & e_1\left(a_2 + b_2\hat{Y}\right)\hat{Y} & 0 \end{bmatrix}.$$

Thus, the eigenvalues of $M(P_{CY}, \hat{r})$ are determined by $\hat{\lambda}_{31}, \hat{\lambda}_{33} = \frac{-(d_1+a_1\hat{Y})\pm\sqrt{(d_1+a_1\hat{Y})^2-4a_1{}^2e_2\hat{Y}\hat{C}}}{2}$, and $\hat{\lambda}_{32} = 0$.

Define $\widehat{\boldsymbol{v}} = (\hat{v}_{31}, \hat{v}_{32}, \hat{v}_{33})^T$, and $\widehat{\boldsymbol{\psi}} = (\hat{\psi}_{31}, \hat{\psi}_{32}, \hat{\psi}_{33})^T$ as the eigenvectors corresponding to $\hat{\lambda}_{32} = 0$ for $M(P_{CY}, \hat{r})$, and $[M(P_{CY}, \hat{r})]^T$ respectively, then it is reached that $\widehat{\boldsymbol{v}} = \left(-\frac{e_1(a_2+b_2\hat{Y})}{e_2a_1}, 1, \frac{e_1(a_2+b_2\hat{Y})(d_1+a_1\hat{Y})}{e_2a_1^2\hat{C}}\right)^T$, and $\widehat{\boldsymbol{\psi}} = (0,1,0)^T$.

Furthermore, direct calculation using Eq. (9) shows that:

$$\frac{\partial F}{\partial r} = F_r = \left(0, \frac{X}{1+hY}, 0\right)^T \Rightarrow \widehat{\boldsymbol{\psi}}^T[F_r(P_{CY}, \hat{r})] = 0.$$

$$\widehat{\boldsymbol{\psi}}^T[DF_r(P_{CY}, \hat{r})\widehat{\boldsymbol{v}}] = \frac{1}{1+h\hat{Y}}.$$

$$\widehat{\boldsymbol{\psi}}^T[D^2F(P_{CY}, \hat{r})(\widehat{\boldsymbol{v}}, \widehat{\boldsymbol{v}})] = -2b_1 - 2\left(\frac{rh}{(1+h\hat{Y})^2} + a_2 + 2b_2\hat{Y}\right)\left(\frac{e_1(a_2+b_2\hat{Y})(d_1+a_1\hat{Y})}{e_2a_1^2\hat{C}}\right).$$

Now, if the condition (17) holds, then according to Sotomayor's theorem, there is a transcritical bifurcation. Otherwise, an application to Eq. (10) shows that:

$$\widehat{\boldsymbol{\psi}}^T[D^3F(P_{CY}, \hat{r})(\widehat{\boldsymbol{v}}, \widehat{\boldsymbol{v}}, \widehat{\boldsymbol{v}})] = \frac{6(h^2r-(1+h\hat{Y})^3b_2)}{(1+h\hat{Y})^3}\left(\frac{e_1(a_2+b_2\hat{Y})(d_1+a_1\hat{Y})}{e_2a_1^2\hat{C}}\right)^2 \neq 0.$$

Thus, according to Sotomayor's theorem, a pitchfork bifurcation occurs.

Theorem 5: For the cohabitation equilibrium point $P_* = (C_*, X_*, Y_*)$:

1) P_* is locally asymptotically stable if the condition (18) is satisfied.
2) When the condition (19) holds, then P_* becomes a globally asymptotically stable.
3) If the conditions (20)-(21) are satisfied, system (2) undergoes a saddle-node bifurcation (SNB) near P_* if the parameter b_1 travels via the value $b_1^* = \frac{\omega_{11}\omega_{23}\omega_{32}}{(-\omega_{11}\omega_{33}+\omega_{13}\omega_{31})X^*}$.

$$\left.\begin{array}{l}\min\{-\omega_{11}, -\omega_{22}\} > 2\omega_{33} \\ \omega_{11}\omega_{33} - \omega_{13}\omega_{31} > 0 \\ \omega_{22}\omega_{33} - \omega_{23}\omega_{32} > 0\end{array}\right\}. \quad (18)$$

$$\left.\begin{array}{c} e_1Y_* < b_1 \\ e_1a_2\bar{\bar{X}} + e_2a_1\bar{\bar{C}} + e_1b_2\bar{\bar{X}}\left(\bar{\bar{Y}} + Y_*\right) + \left(rh + b_2\bar{\bar{Y}}\right)^2 < d_3\end{array}\right\}, \quad (19)$$

where $\bar{\bar{C}}$, $\bar{\bar{X}}$, and $\bar{\bar{Y}}$ are the upper bounds of each variable according to Theorem 1.

$$2b_2Y_* > \frac{rh}{(1+hY_*)^2} + a_2. \quad (20)$$

$$-\frac{\omega_{31}}{\omega_{11}}c_{11}(P_*, b_1^*) - \frac{\omega_{32}}{\omega_{22}}c_{21}(P_*, b_1^*) + c_{31}(P_*, b_1^*) \neq 0. \quad (21)$$

Here, ω_{ij} for $i,j = 1,2,3$ are given in the proof, while c_{11}, c_{21}, and c_{31} are the coefficients of

the vector given by equation (9).

Proof: **(1)** For the cohabitation equilibrium, the matrix (8) becomes:

$$M(P_*)=\begin{bmatrix}-(d_1+a_1Y_*) & 0 & -a_1C_* \\ 0 & -b_1X_* & -X_*\left(\frac{rh}{(1+hY_*)^2}+a_2+2b_2Y_*\right) \\ e_2a_1Y_* & Y_*\big(e_1(a_2+b_2Y_*)\big) & e_1b_2X_*Y_*\end{bmatrix}=[\omega_{ij}]. \quad (22)$$

The following is the characteristic equation for $M(P_*)$:

$$\lambda^3+A_1\lambda^2+A_2\lambda+K=0, \quad (23)$$

where:

$$A_1=-(\omega_{11}+\omega_{22}+\omega_{33}).$$
$$A_2=\omega_{11}\omega_{22}+\omega_{11}\omega_{33}+\omega_{22}\omega_{33}-\omega_{23}\omega_{32}-\omega_{13}\omega_{31}.$$
$$K=-(\omega_{11}\omega_{22}\omega_{33}-\omega_{11}\omega_{23}\omega_{32}-\omega_{22}\omega_{13}\omega_{31}).$$

With

$$\Delta=A_1A_2-K=-\omega_{11}\omega_{22}(\omega_{11}+\omega_{22})-(\omega_{11}+\omega_{33})[\omega_{11}\omega_{33}-\omega_{13}\omega_{31}] \\ -(\omega_{22}+\omega_{33})[\omega_{22}\omega_{33}-\omega_{23}\omega_{32}]-2\omega_{11}\omega_{22}\omega_{33}.$$

Thus, by utilizing the Routh-Hurwitz criterion, which requires $A_1>0$, $K>0$, and $\Delta>0$, the result is reached under the condition (18), and hence P_* is a local asymptotic stability.

(2) Consider the real valued function $\mho_4=l_4\frac{1}{2}(C-C_*)^2+l_5\left(X-X_*-X_*ln\frac{X}{X_*}\right)+l_6\frac{1}{2}(Y-Y_*)^2$, with $l_i, i=4,5,6$ are positive constants. Simple calculation explains that $\mho_4: U_4\to\mathbb{R}$, where $U_4=\{(C,X,Y)\in\mathbb{R}^3_+, C\geq 0, X>0, Y\geq 0\}$, so that $\mho_4(P_*)=0$ and $\mho_4(C,X,Y)>0$, $\forall\,(C,X,Y)\in U_4-P_*$. Furthermore, direct calculation leads to:

$$\frac{d\mho_4}{dT}=l_4(C-C_*).\frac{dC}{dT}+l_5\frac{(X-X_*)}{X}\frac{dX}{dT}+l_6(Y-Y_*)\frac{dY}{dT}.$$

Therefore, it is obtained that:

$$\frac{d\mho_4}{dT}=-l_4(d_1+a_1Y_*)(C-C_*)^2-l_5b_1(X-X_*)^2 \\ -l_6[d_3-e_1a_2X-e_2a_1C-e_1b_2X(Y+Y_*)](Y-Y_*)^2 \\ -a_1[l_4C-l_6e_2Y_*](C-C_*)(Y-Y_*) \\ -\left(l_5\left(\frac{rh}{1+hY}+a_2+b_2Y+b_2Y_*\right)-l_6e_1Y_*(a_2+b_2Y_*)\right)(X-X_*)(Y-Y_*).$$

Selecting $l_4=\frac{e_2Y_*}{C}$, $l_5=e_1Y_*$, and $l_6=1$ yields that:

$$\frac{d\mho_4}{dT} \leq -\frac{e_2 Y_*}{C}(d_1 + a_1 Y_*)(C - C_*)^2 - e_1 Y_*(b_1 - e_1 Y_*)(X - X_*)^2$$
$$-\left(d_3 - e_1 a_2 X - e_2 a_1 C - e_1 b_2 X(Y + Y_*) - \left(\frac{rh}{1 + hY} + b_2 Y\right)^2\right)(Y - Y_*)^2.$$

Thus, condition (19) leads to $\frac{d\mho_4}{dT} < 0$. Accordingly, P_* is globally asymptotically stable.

(3) Substituting the value of $b_1 = b_1^*$, which is positive under condition (20), in the matrix (22), then its characteristic equation (23) reduces to $\lambda[\lambda^2 + A_1\lambda + A_2] = 0$, as the value of K became $K = 0$.

Thus, the eigenvalues become $\lambda_{*1} = 0$, and $\lambda_{*2}, \lambda_{*3} = \frac{-A_1 \pm \sqrt{A_1^2 - 4A_2}}{2}$. This makes P_* a nonhyperbolic equilibrium point when $b_1 = b_1^*$. Sotomayer's theorem is now used to identify the saddle-node bifurcation.

Define $\boldsymbol{v}_* = (v_{41}, v_{42}, v_{43})^T$, and $\boldsymbol{\psi}_* = (\psi_{41}, \psi_{42}, \psi_{43})^T$ as the eigenvectors corresponding to $\lambda_{*1} = 0$ for $M(P_*, b_1^*)$, and $[M(P_*, b_1^*)]^T$ respectively. Then it is reached to: $\boldsymbol{v}_* = \left(-\frac{\omega_{13}}{\omega_{11}}, -\frac{\omega_{23}}{\omega_{22}}, 1\right)^T$, and $\boldsymbol{\psi}_* = (-\frac{\omega_{31}}{\omega_{11}}, -\frac{\omega_{32}}{\omega_{22}}, 1)^T$.

Furthermore, simple computation using Eq. (9) leads to:

$$\frac{\partial F}{\partial b_1} = F_{b_1} = (0, -X^2, 0)^T \;\Rightarrow\; \boldsymbol{\psi}_*{}^T[F_{b_1}(P_*, b_1^*)] = \frac{\omega_{32}}{\omega_{22}} X_*^2 \neq 0.$$

$$\boldsymbol{\psi}_*{}^T[D^2 F(P_*, b_1^*)(\boldsymbol{v}_*, \boldsymbol{v}_*)] = -\frac{\omega_{31}}{\omega_{11}} c_{11}(P_*, b_1^*) - \frac{\omega_{32}}{\omega_{22}} c_{21}(P_*, b_1^*) + c_{31}(P_*, b_1^*).$$

Therefore, according to Sotomayor's theorem, there is an SNB under condition (21).

4. PERSISTENCE

Understanding persistence in ecological systems is essential to comprehending how, over time, ecosystems preserve their biodiversity, structure, and function in spite of disturbances and environmental changes. As a result, system (2) can drive two subsystems. They are portrayed as follows:

The first Subsystem is written as:

$$\left.\begin{aligned} \frac{dC}{dT} &= \Lambda - d_1 C = f_1(C, X, Y) = h_1(C, X) \\ \frac{dX}{dT} &= X(r - d_2 - b_1 X) = h_2(C, X) \end{aligned}\right\}. \tag{24}$$

While the second subsystem is written as:

$$\left.\begin{array}{l}\frac{dC}{dT} = \Lambda - d_1 C - a_1 CY = g_1(C,Y) \\ \frac{dY}{dT} = Y(e_2 a_1 C - d_3) = g_2(C,Y)\end{array}\right\}. \tag{25}$$

The Dulac functions $B_1(C,X) = \frac{1}{X}$ and $B_2(C,Y) = \frac{1}{Y}$, which fulfill $B_i > 0,\ i = 1,2$ and have continuous first derivative functions in the $int\ \mathbb{R}_+^2$ of the boundary planes, are considered. Therefore, straightforward calculation demonstrates that

$$\Delta(C,X) = \frac{\partial B_1 h_1}{\partial C} + \frac{\partial B_1 h_2}{\partial X} = -\frac{d_1}{X} - \mathrm{b}_1 < 0.$$

$$\Delta(C,Y) = \frac{\partial B_2 g_1}{\partial C} + \frac{\partial B_2 g_2}{\partial X} = -\frac{d_1}{Y} - \mathrm{a}_1 < 0.$$

Then $\Delta(C,X)$, and $\Delta(C,Y)$ do not determine zero in the $int\ \mathbb{R}_+^2$ of their planes and do not change their sign.

According to the Dulac-Bendixson criterion [32], there is therefore no closed curve in the $int\ \mathbb{R}_+^2$ of the boundary

planes. Furthermore, a single equilibrium point in the $int\ \mathbb{R}_+^2$ of the above subsystems defined by P_{CX} and P_{CY} is globally asymptotically stable whenever it is locally stable, according to the Poincaré-Bendixson theorem [32].

Theorem 6: If the next requirements are satisfactory, the system (2) becomes uniformly persistent:

$$\left.\begin{array}{c} d_2 < r \\ or \\ d_3 d_1 < e_2 a_1 \Lambda \end{array}\right\} \tag{26}$$

$$d_3 < e_1 a_2 \bar{X} + e_2 a_1 \bar{C}. \tag{27}$$

$$\left[d_2 + \left(a_2 + b_2 \hat{Y}\right)\hat{Y}\right]\left(1 + h\hat{Y}\right) < r. \tag{28}$$

Proof: According to the average Lyapunov function technique [33], let $\varphi(C,X,Y) = C^{q_1} X^{q_2} Y^{q_3}$, where $q_i > 0, \forall i = 1,2,3$ are constants. Hence, for every $(C,X,Y) \in int\ \mathbb{R}_+^3$, $\varphi(C,X,Y) \to 0$, when one of their variables gets close to zero.

In addition, it is computed that

$$\Omega(C,X,Y) = \frac{\varphi'(C,X,Y)}{\varphi(C,X,Y)} = \frac{q_1}{C} f_1 + q_2 f_2 + q_3 f_3.$$

The equilibrium points P_C, P_{CX}, and P_{CY} are the sole potential omega limit sets of system (2) because the boundary planes lack periodic attractors. Therefore, if we can demonstrate that $\Omega(.) > 0$ at each of these locations, the system is uniformly persistent. Additionally, we have:

$$\Omega(P_C) = q_2(r - d_2) + q_3\left(e_2 a_1 \frac{\Lambda}{d_1} - d_3\right).$$

$$\Omega(P_{CX}) = q_3(e_1a_2\bar{X} + e_2a_1\bar{C} - d_3).$$

$$\Omega(P_{CY}) = q_2\left(\frac{r}{1+h\hat{Y}} - d_2 - (a_2 + b_2\hat{Y})\hat{Y}\right).$$

Note that, $\Omega(P_C) > 0$ for an appropriate selection of $q_i, i = 2,3$, under the conditions (26). Furthermore, $\Omega(P_{CX}) > 0$ and $\Omega(P_{CY}) > 0$ when the requirements (27) and (28) are met, respectively. Hence, the uniformly persistent occurs.

5. NUMERICAL SIMULATION

To better understand the global dynamics of the proposed system, and in particular the control set of parameters, an extensive numerical simulation of system (2) is carried out in this section. System (2) was solved using MATLAB version R2021a and the Runge-Kutta of order four scheme. The numerical results are then displayed as a 2D time series and a 3D phase picture with the following fictitious set of parameters. It should be noted that the equilibrium points are symbolized by the red dots in the following pictures, whilst the blue dots represent various initial positions.

$$\Lambda = 2, d_1 = 0.1, a_1 = 0.2, r = 2, h = 0.2, d_2 = 0.15, b_1 = 0.2, a_2 = 0.1, \\ b_2 = 0.02, e_1 = 0.1, e_2 = 0.25, d_3 = 0.2 \quad . \tag{29}$$

Figure 1 illustrates how, using the data set (29), system (2) asymptotically approaches the cohabitation equilibrium point $P_* = (2.95, 3.31, 2.88)$ from a variety of initial values.

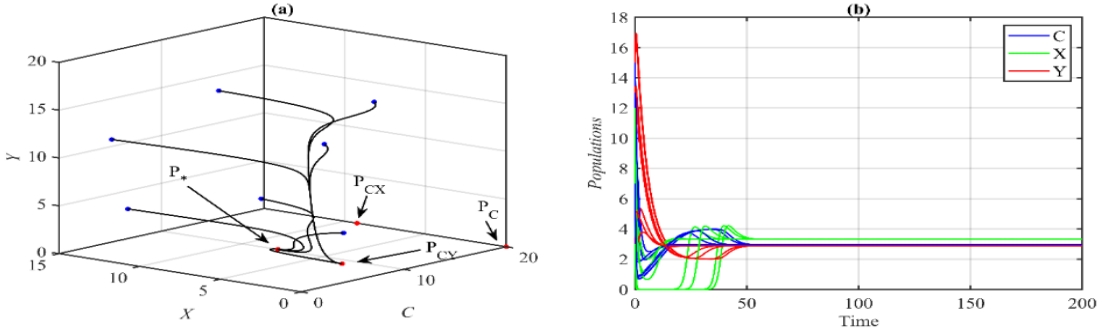

Fig. 1: The data set (29) is used to solve system (2) from various initial points. (a) All solutions asymptotically approach $P_* = (2.95, 3.31, 2.88)$; (b) The solutions in relation with time.

Figure 1 shows that although the other boundary equilibrium points of systems are unstable, system (2) possesses a globally stable cohabitation equilibrium point.

It is observed that, for $\Lambda \leq 0.2$, the trajectories are approaching P_{CX}. However, for $\Lambda \geq 4.1$, they approach P_{CY}. Otherwise, the trajectories approach P_*, see Figure 2.

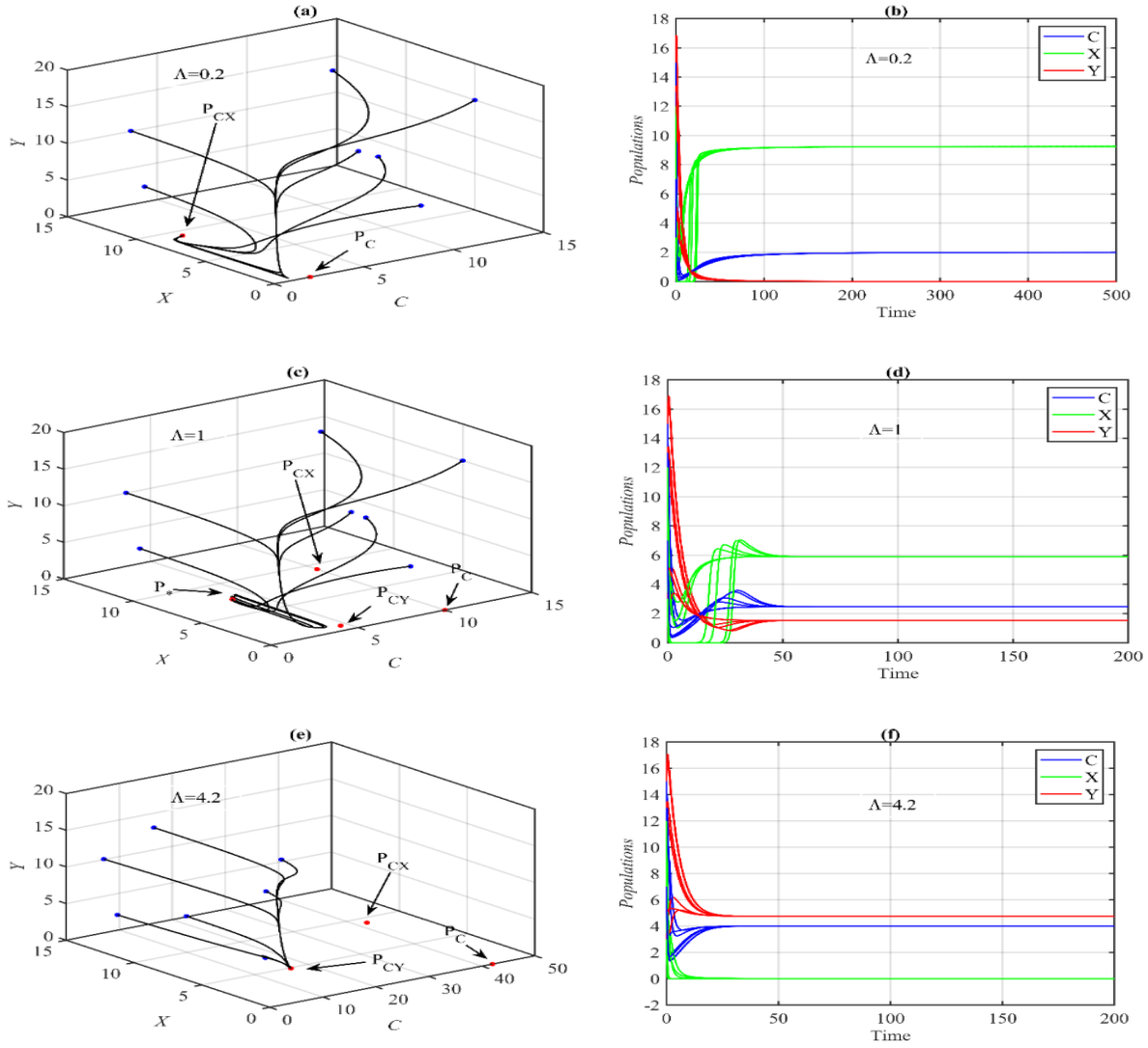

Fig. 2: The data set (29), with selected values of $\Lambda = 0.2, 1, 4.2$, respectively, is used to solve system (2) from various initial points. (a) When $\Lambda = 0.2$, every trajectory approaches $P_{CX} = (1.99,9.24,0)$; (c) When $\Lambda = 1$, every trajectory approaches $P_* = (2.45,5.89,1.53)$; (e) When $\Lambda = 4.2$, every trajectory approaches $P_{CY} = (4, 0, 4.74)$; (b, d, f) The solutions in relation with time for $\Lambda = 0.2, 1, 4.2$, respectively.

Consequently, the carrion-eater will go extinct if the value of Λ is lowered below a critical value, and the prey will go extinct if it is raised above another critical value. Otherwise, the system remains persistent by maintaining a balance between their values between these two crucial values. It was also noted that parameter e_2 has an effect similar to the Λ effect on the dynamics of System (2).

It is observed that, for $a_1 \leq 0.02$, the trajectories are approaching P_{CX}. Otherwise, the trajectories approach P_*, see Figure 3.

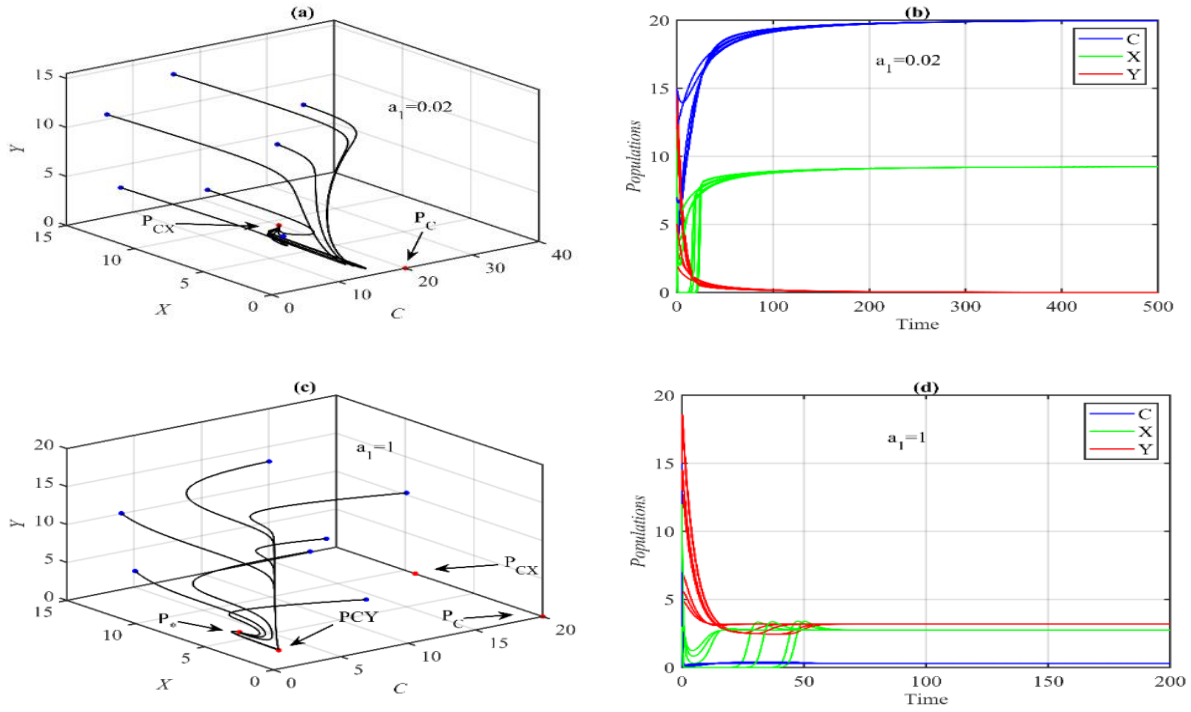

Fig. 3: The data set (29), with selected values of $a_1 = 0.02, 1,$ respectively, is used to solve system (2) from various initial points. (a) When $a_1 = 0.02$, every trajectory approaches $P_{CX} = (19.97, 9.23, 0)$; (c) When $a_1 = 1$, every trajectory approaches $P_* = (0.3, 2.76, 3.17)$; (b, d) The solutions in relation to time for $a_1 = 0.02, 1,$ respectively.

Clearly, Figure 3 shows that the carrion-eater will go extinct if the value of a_1 is lowered below a critical value. Otherwise, the system remains persistent. Moreover, it is observed that, for $r \leq 0.6$, the trajectories are approaching P_{CY}. Otherwise, the trajectories approach P_*, see Figure 4.

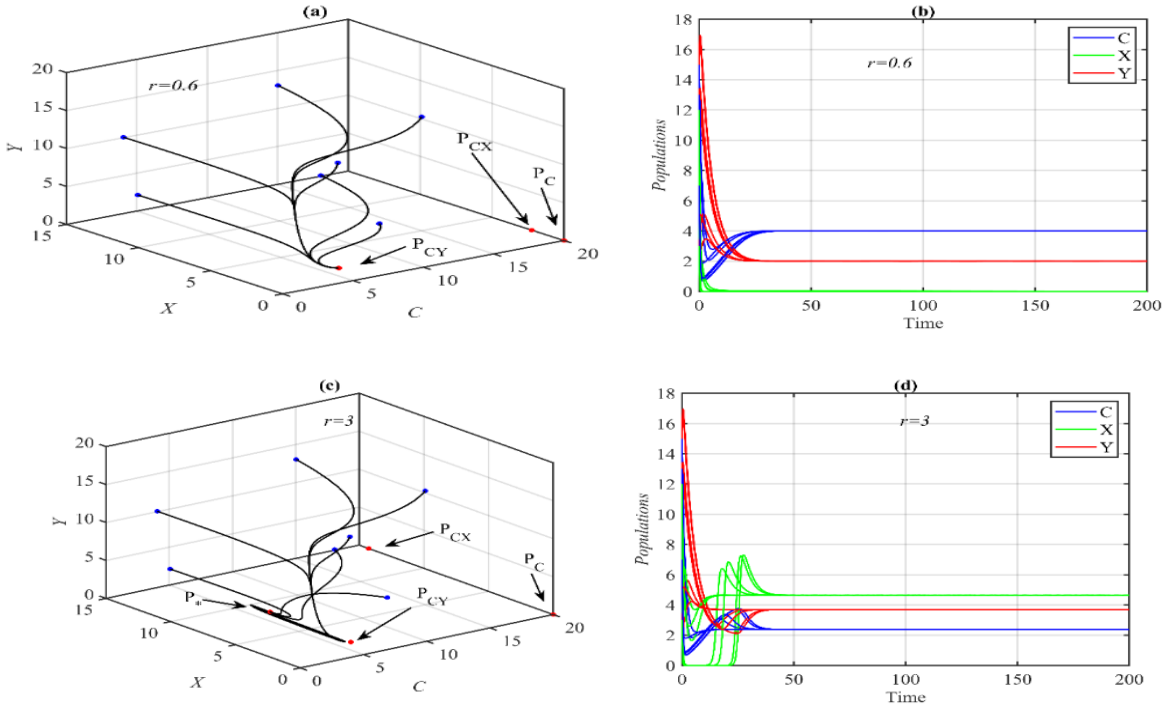

Fig. 4: The data set (29), with selected values of $r = 0.6, 3,$ respectively, is used to solve system (2) from various initial points. (a) When $r = 0.6$, every trajectory approaches $P_{CY} = (3.99, 0, 2)$; (c) When $r = 3$, every trajectory approaches $P_* = (2.38, 4.65, 3.69)$; (b, d) The solutions in relation with time for $r = 0.6, 3,$ respectively.

Keep in mind that Figure 4 shows that the prey will go extinct if the value of r is lowered below a critical value. Otherwise, the system remains persistent. Furthermore, it was also noted that parameter d_3 has an effect similar to the r effect on the dynamics of System (2).

Now Figure 5 shows that the prey will go extinct if the value of h becomes $h \geq 1.7$. Otherwise, the system remains persistent.

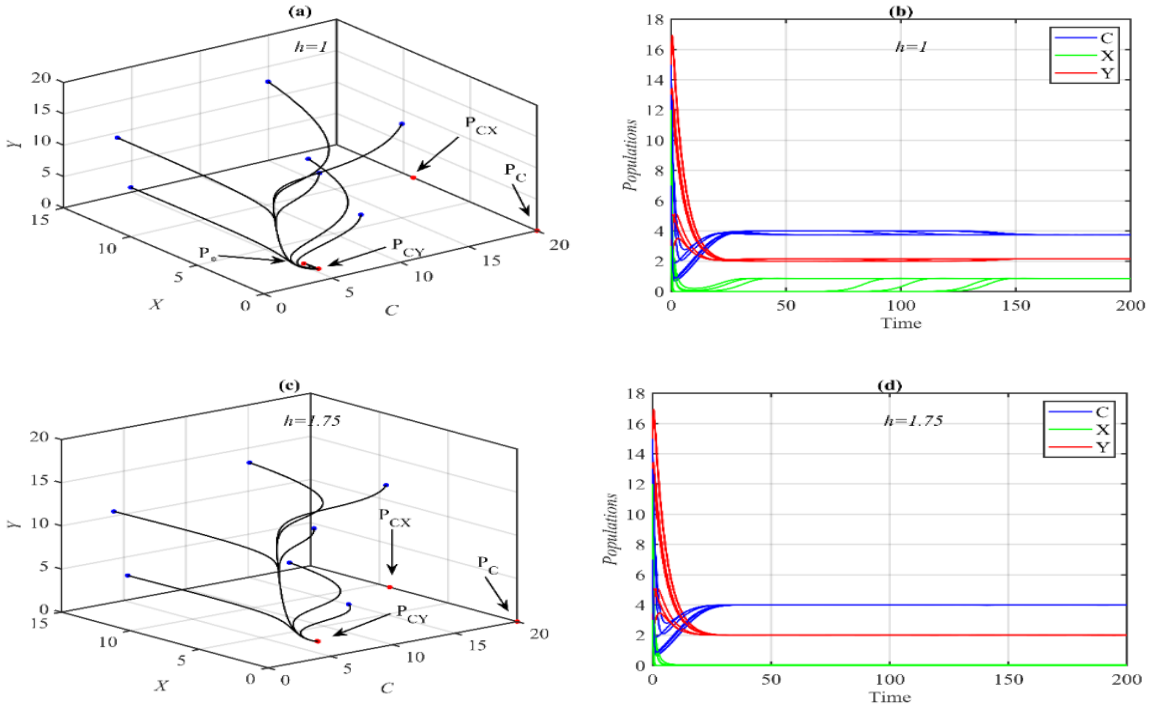

Fig. 5: The data set (29), with selected values of $h = 1, 1.75,$ respectively, is used to solve system (2) from various initial points. (a) When $h = 1$, every trajectory approaches $P_* = (3.75, 0.85, 2.16)$; (c) When $h = 1.75$, every trajectory approaches $P_{CY} = (3.99, 0, 2)$; (b, d) The solutions in relation with time for $h = 1, 1.75,$ respectively.

According to Figure 5, the prey faces extinction when the value of h becomes larger than 1.7; otherwise, the system is still persistent. It is also noted that the parameters a_2 and b_2 have a similar impact on the dynamics of system (2) as shown with varying h.

Lastly, it is observed that, for the data set (29), changing one of the parameters d_1, d_2, b_1, and e_1 each time has a quantifiable effect on the dynamics of the system (2). However, when they vary more than one at the same time, they clearly have a qualitative impact; see Figure 6, which uses data (29) with $d_1 = 0.6$, $r = 0.5$, and $d_2 = 0.65$.

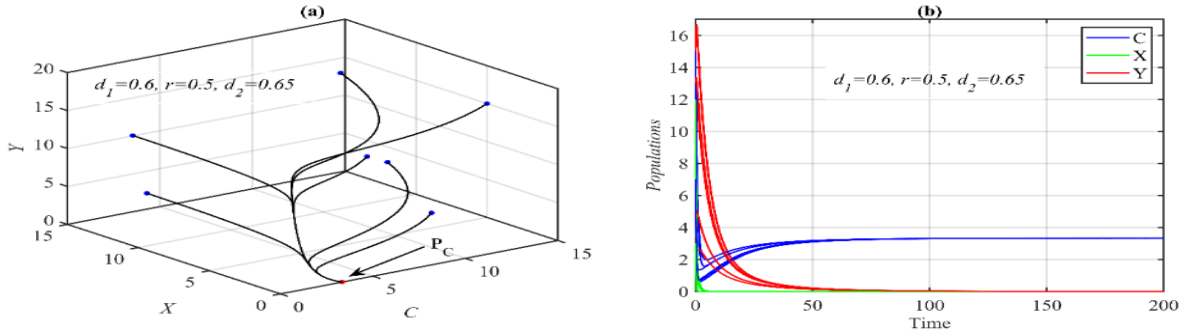

Fig. 6: The data set (29), with $d_1 = 0.6$, $r = 0.5$, and $d_2 = 0.65$, is used to solve system (2) from various initial points. (a) Every trajectory approaches $P_C = (3.33, 0, 0)$; (b) The solutions in relation to time.

It is easy to verify that the data used in Figure 6 satisfies the condition (11) of Theorem 2.

6. CONCLUSION

This research proposed and examined the carcasses-prey-carrion-eater system in the context of the group's hunting. The maximum number of equilibrium points is found to be four. Every prerequisite for their persistence, bifurcation, and stability is identified. While the group's hunting results in bistable or periodic dynamics, the suggested system lacks the periodic dynamics inherent in a prey-predator system and simply has a point attractor. This suggests that the presence of carcasses in the habitat regulated the dynamics between prey and predators. Additionally, the numerical simulation yields the following results, even though it validates the findings we arrived at. The existence of carcasses in the environment stabilizes the prey-predator system by removing cyclic movement. The durability of the system (2) is positively correlated with the assault rate of carcasses, the birth rate of prey, and the death rate of carrion-eaters. However, there is a negative proportionality between the system's (2) persistence and the Carrion-eater's panic level, attack rate, and the group's hunting rate.

When comparing the results of this research with those in [1], it was noted that the presence of the group's hunting, rather than a predator-dependent refuge, does not change the dynamic behavior in the border areas, whereas there is a fundamental change in the first positive octant. It was observed for both models that the presence of carrion in the environment stabilizes the prey-predator system, while the group-hunting mechanism significantly affects the nature of the stability and persistence of the system.

CONFLICT OF INTERESTS

The authors declare that there is no conflict of interests.

REFERENCES

[1] S. Al-Momen, R.K. Naji, The Dynamics of Sokol-Howell Prey-Predator Model Involving Strong Allee Effect, Iraqi J. Sci. 62 (2021), 3114-3127. https://doi.org/10.24996/ijs.2021.62.9.27.

[2] M. Barbier, L. Wojcik, M. Loreau, A Macro-Ecological Approach to Predation Density-Dependence, Oikos 130 (2021), 553-570. https://doi.org/10.1111/oik.08043.

[3] J.D. Murray, Mathematical Biology, Springer, New York, 2002. https://doi.org/10.1007/b98868.

[4] F.H. Maghool, R.K. Naji, Chaos in the Three-Species Sokol-Howell Food Chain System with Fear, Commun. Math. Biol. Neurosci. 2022 (2022), 14. https://doi.org/10.28919/cmbn/7056.

[5] K. Sarkar, S. Khajanchi, Impact of Fear Effect on the Growth of Prey in a Predator-Prey Interaction Model, Ecol. Complex. 42 (2020), 100826. https://doi.org/10.1016/j.ecocom.2020.100826.

[6] K.A. Amri, Q.J.A. Khan, D. Greenhalgh, Combined Impact of Fear and Allee Effect in Predator-Prey Interaction Models on Their Growth, Math. Biosci. Eng. 21 (2024), 7211-7252. https://doi.org/10.3934/mbe.2024319.

[7] X. Wang, L. Zanette, X. Zou, Modelling the Fear Effect in Predator–Prey Interactions, J. Math. Biol. 73 (2016), 1179-1204. https://doi.org/10.1007/s00285-016-0989-1.

[8] X. Wang, X. Zou, Modeling the Fear Effect in Predator–Prey Interactions with Adaptive Avoidance of Predators, Bull. Math. Biol. 79 (2017), 1325-1359. https://doi.org/10.1007/s11538-017-0287-0.

[9] S.A. Rahi, R.K. Naji, The Role of Fear and Competition in the Dynamic of the Prey-Predator-Scavenger System, Ain Shams Eng. J. 16 (2025), 103494. https://doi.org/10.1016/j.asej.2025.103494.

[10] S. Samaddar, M. Dhar, P. Bhattacharya, Effect of Fear on Prey–Predator Dynamics: Exploring the Role of Prey Refuge and Additional Food, Chaos 30 (2020), 063129. https://doi.org/10.1063/5.0006968.

[11] H. Zhang, Y. Cai, S. Fu, W. Wang, Impact of the Fear Effect in a Prey-Predator Model Incorporating a Prey Refuge, Appl. Math. Comput. 356 (2019), 328-337. https://doi.org/10.1016/j.amc.2019.03.034.

[12] N.H. Fakhry, R.K. Naji, Fear and Hunting Cooperation's Impact on the Eco-Epidemiological Model's Dynamics, Int. J. Anal. Appl. 22 (2024), 15. https://doi.org/10.28924/2291-8639-22-2024-15.

[13] M.J. Hansen, P. Domenici, P. Bartashevich, A. Burns, J. Krause, Mechanisms of Group-Hunting in Vertebrates, Biol. Rev. 98 (2023), 1687-1711. https://doi.org/10.1111/brv.12973.

[14] R.K. Naji, Contribution of Hunting Cooperation and Antipredator Behavior to the Dynamics of the Harvested Prey-Predator System, Commun. Math. Biol. Neurosci. 2023 (2023), 99. https://doi.org/10.28919/cmbn/8164.

[15] D. Abid, R.K. Naji, The Role of Fear and Predator-Dependent Refuge on the Dynamics of the Carcasses-Prey-Scavenger System, Commun. Math. Biol. Neurosci. 2025 (2025), 145. https://doi.org/10.28919/cmbn/9578.

[16] J.G. Clapp, J.L. Malmberg, J.D. Holbrook, Examining Pathogen Avoidance in Predator-Prey and Scavenging Systems, Front. Ecol. Evol. 12 (2024), 1481290. https://doi.org/10.3389/fevo.2024.1481290.

[17] A. Luna, P. Romero-Vidal, E. Arrondo, Predation and Scavenging in the City: A Review of Spatio-Temporal Trends in Research, Diversity 13 (2021), 46. https://doi.org/10.3390/d13020046.

[18] A.Q. Khan, S.S. Kazmi, T.D. Alharbi, Bifurcations of a Three-Species Prey-Predator System with Scavenger, Ain Shams Eng. J. 14 (2023), 102514. https://doi.org/10.1016/j.asej.2023.102514.

[19] M.J. Le Sage, B.D. Towey, J.L. Brunner, Do Scavengers Prevent or Promote Disease Transmission? The Effect of Invertebrate Scavenging on Ranavirus Transmission, Funct. Ecol. 33 (2019), 1342-1350. https://doi.org/10.1111/1365-2435.13335.

[20] M. Moleón, J.A. Sánchez-Zapata, The Role of Carrion in the Landscapes of Fear and Disgust: A Review and Prospects, Diversity 13 (2021), 28. https://doi.org/10.3390/d13010028.

[21] J. Tobajas, E. Descalzo, P. Ferreras, R. Mateo, A. Margalida, Effects on Carrion Consumption in a Mammalian Scavenger Community when Dominant Species Are Excluded, Mamm. Biol. 101 (2021), 851-859. https://doi.org/10.1007/s42991-021-00163-w.

[22] E.E. Wilson, E.M. Wolkovich, Scavenging: How Carnivores and Carrion Structure Communities, Trends Ecol. Evol. 26 (2011), 129-135. https://doi.org/10.1016/j.tree.2010.12.011.

[23] D. Bai, J. Tang, Global Dynamics of a Predator–Prey System with Cooperative Hunting, Appl. Sci. 13 (2023), 8178. https://doi.org/10.3390/app13148178.

[24] K.M. Gaynor, J.S. Brown, A.D. Middleton, M.E. Power, J.S. Brashares, Landscapes of Fear: Spatial Patterns of Risk Perception and Response, Trends Ecol. Evol. 34 (2019), 355-368. https://doi.org/10.1016/j.tree.2019.01.004.

[25] R. van Klink, J. van Laar-Wiersma, O. Vorst, C. Smit, Rewilding with Large Herbivores: Positive Direct and Delayed Effects of Carrion on Plant and Arthropod Communities, PLoS One 15 (2020), e0226946. https://doi.org/10.1371/journal.pone.0226946.

[26] Y. Du, B. Niu, J. Wei, A Predator-Prey Model with Cooperative Hunting in the Predator and Group Defense in the Prey, Discrete Contin. Dyn. Syst. Ser. B 27 (2022), 5845. https://doi.org/10.3934/dcdsb.2021298.

[27] S. Pal, N. Pal, S. Samanta, J. Chattopadhyay, Fear Effect in Prey and Hunting Cooperation among Predators in a Leslie-Gower Model, Math. Biosci. Eng. 16 (2019), 5146-5179. https://doi.org/10.3934/mbe.2019258.

[28] B. Habib, S. Gwal, T. Singh, R. Ghade, D. Miranda, et al., Habitat Suitability and Connectivity for Clouded Leopard Neofelis nebulosa in Northeast India, Sci. Rep. 15 (2025), 33373. https://doi.org/10.1038/s41598-025-17900-7.

[29] S.L. Bartel, T. Stephenson, D.W. Crowder, M.E. Jones, A. Storfer, et al., Global Change Influences Scavenging and Carrion Decomposition, Trends Ecol. Evol. 39 (2024), 152-164. https://doi.org/10.1016/j.tree.2023.09.008.

[30] A. Inagaki, M.L. Allen, S. Koike, Integration of Specific Metrics Can Promote the Understanding of Scavenging Dynamics, Front. Ecol. Evol. 13 (2025), 1611982. https://doi.org/10.3389/fevo.2025.1611982.

[31] F. Chen, On a Nonlinear Nonautonomous Predator–Prey Model with Diffusion and Distributed Delay, J. Comput. Appl. Math. 180 (2005), 33-49. https://doi.org/10.1016/j.cam.2004.10.001.

[32] L. Perko, Differential Equations and Dynamical Systems, Springer, 2001.

[33] T.C. Gard, Uniform Persistence in Multispecies Population Models, Math. Biosci. 85 (1987), 93-104. https://doi.org/10.1016/0025-5564(87)90101-5.